AS REVISED: Revision #1

Ophirite, $Ca_2Mg_4[Zn_2Mn^{3+}{}_2(H_2O)_2(Fe^{3+}W_9O_{34})_2]\bullet 46H_2O$, a new mineral with a heteropolytungstate tri-lacunary Keggin anion

ANTHONY R. KAMPF[1§], JOHN M. HUGHES[2], BARBARA P. NASH[3], STEPHEN E. WRIGHT[4], GEORGE R. ROSSMAN[5], JOE MARTY[6]

[1]Mineral Sciences Department, Natural History Museum of Los Angeles County, Los Angeles, CA 90007, U.S.A.
[2]Department of Geology, University of Vermont, Burlington, VT 05405, U.S.A.
[3]Department of Geology and Geophysics, University of Utah, Salt Lake City, Utah 84112, U.S.A.
[4]Department of Statistics, Miami University, Oxford, OH 45056, U.S.A.
[5]Division of Geological and Planetary Sciences, California Institute of Technology, Pasadena, CA 91125, U.S.A.
[6]5199 E. Silver Oak Rd., Salt Lake City, UT 84108, U.S.A.

ABSTRACT

Ophirite, $Ca_2Mg_4[Zn_2Mn^{3+}{}_2(H_2O)_2(Fe^{3+}W_9O_{34})_2]\bullet 46H_2O$, is a new mineral species from the Ophir Hill Consolidated mine, Ophir District, Oquirrh Mountains, Tooele County, Utah, U.S.A. Crystals of ophirite are orange-brown tablets on {001} with irregular {100} and {110} bounding forms; individual crystals are up to about 1 mm in maximum dimension and possess a pale orange streak. The mineral is transparent, with a vitreous luster; it does not fluoresce in short- or long-wave ultraviolet radiation. Ophirite has a Mohs hardness of approximately 2 and brittle tenacity. No cleavage or parting was observed in the mineral. The fracture is irregular. The density calculated from the empirical formula using the single-crystal cell data is 4.060 g•cm^{-3}. Ophirite is biaxial (+) with a $2V$ angle of 43(2)º. Indices of refraction for ophirite are α 1.730(3), β 1.735(3), γ 1.770(3). The optic orientation (incompletely determined) is Y ^ **b** ≈ 9° and one

§ Email: akampf@nhm.org

optic axis is approximately perpendicular to {001}. Dispersion $r > v$, strong; pleochroism is X = light orange brown, Y = light orange brown, Z = orange brown; $X < Y << Z$. Chemical analyses of ophirite were obtained by electron probe microanalysis; optimization of that analysis using the results of the crystal structure analysis yielded the formula $(Ca_{1.46}Mg_{0.50}Zn_{0.04})_{\Sigma 2.00}(Mg_{3.96}Mn^{3+}_{0.04})_{\Sigma 4.00}[(Zn_{1.16}Fe^{3+}_{0.68}Ca_{0.14}Sb^{5+}_{0.02})_{\Sigma 2.00}(Mn^{3+}_{1.42}Sb^{5+}_{0.32}Fe^{3+}_{0.24}W_{0.02})_{\Sigma 2.00}[(H_2O)_2((Fe^{3+}_{0.80}Sb^{5+}_{0.11}Ca_{0.07}Mg_{0.02})_{\Sigma 1.00}(W_{8.71}Mn^{3+}_{0.29})_{\Sigma 1.00})_2]]\bullet 46H_2O$; the simplified formula of ophirite is $Ca_2Mg_4[Zn_2Mn^{3+}_2(H_2O)_2(Fe^{3+}W_9O_{34})_2]\bullet 46H_2O$. Ophirite is triclinic, $P\bar{1}$, with a 11.9860(2), b 13.2073(2), c 17.689(1) Å, α 69.690(5), β 85.364(6), γ 64.875(5)° , V 4647.2(4) Å^3, and Z = 1. The strongest four lines in the diffraction pattern are [d in Å(I)(hkl)]: 10.169(100)(100,110), 11.33(91)(011,010), 2.992(75)(334,341,$\bar{1}\,\bar{1}$ 5), and 2.760(55)(412,006, $\bar{1}$ 3 5). The atomic arrangement of ophirite was solved and refined to R_1 = 0.0298 for 9,230 independent reflections. The structural unit, ideally $\{^{[6]}Zn_2{}^{[6]}Mn^{3+}_2(H_2O)_2(^{[4]}Fe^{3+[6]}W^{6+}_9O_{34})_2\}^{12-}$, consists of a $[Zn_2Mn^{3+}_2(H_2O)_2]$ octahedral layer sandwiched between opposing heteropolytungstate tri-lacunary ($^{[4]}Fe^{3+[6]}W^{6+}_9O_{34}$) Keggin anions. Similar structures with an octahedral layer between two tri-lacunary Keggin anions are known in synthetic phases. Charge balance in the ophirite structure is maintained by the $\{[Mg(H_2O)_6]_4[Ca(H_2O)_6]_2\bullet 10H_2O\}^{12+}$ interstitial unit. The interstitial unit in the structure of ophirite is formed of two distinct $Mg(H_2O)_6$ octahedra and a $Ca(H_2O)_6O_1$ polyhedron, as well as five isolated water molecules. The linkage between the structural unit and the interstitial unit results principally from hydrogen bonding between oxygen atoms of the structural unit with hydrogen atoms of the interstitial unit. Ophirite is the first known mineral to contain a lacunary defect derivative of the Keggin anion, a heteropolyanion that is well-known in synthetic phases. The new mineral is named ophirite to recognize its

discovery at the Ophir Hill Consolidated mine, Ophir District, Oquirrh Mountains, Tooele County, Utah, U.S.A.

Keywords: ophirite; new mineral species; heteropolytungstate lacunary Keggin anion; crystal structure; Ophir Hill Consolidated mine, Tooele County, Utah

INTRODUCTION

The Ophir mining district, Utah, was organized shortly after ore deposits were discovered in the Oquirrh Mountains in 1865. For a century, the district was an important source of lead, zinc, copper, and silver ores until the close of the Ophir Hill Consolidated mine in 1972 (Marty and Wise 2007). The geologic setting of the Ophir district is given by those authors, and this brief summary is taken from their work. The Oquirrh Mountains are formed of allochthonous folded and faulted Paleozoic sedimentary rocks; these nappes were transported eastward in the Sevier thrust belt. In the Ophir district, in the southern portion of the Oquirrh Mountains, the sedimentary rocks form an 8,000 ft. sequence that spans the entire Paleozoic, including limestone and dolomite with minor shale and sandstone. Throughout the district there are small intrusions of quartz monzonite porphyry that are spatially related to the ore, and may also be genetically related. Mineralization in the district is confined to a northwest-trending belt less than one mile wide and three miles in length, coincident with the crest of a broad, northwest plunging anticline. The Ophir district had a total production of 2.8 million tons of ore, averaging 6.5% Pb, 1.6% Zn, 0.8% Cu, 7.2 oz per ton Ag, and 0.006 oz per ton Au.

Herein, we describe a new mineral from the Ophir District. The new mineral species was discovered at the Ophir Hill Consolidated mine and is named ophirite in recognition of the type

locality. The new mineral and name were approved by the Commission on New Minerals, Nomenclature and Classification of the International Mineralogical Association (IMA 2013-017). The two cotype specimens used in the description of the mineral are housed in the mineral collection of the Natural History Museum of Los Angeles County under catalogue numbers 64029 and 64030. Ophirite is the first known mineral to contain a lacunary defect derivative of the Keggin anion, a heteropolyanion that is well-known in synthetic phases, and its description introduces that polyanion and its associated structural groups to the mineralogical literature.

OCCURRENCE

Ophirite was found underground at the Ophir Hill Consolidated mine, near a calcite cave known for the presence of micro scheelite crystals. Unlike other mines in the district, the Ophir Hill Consolidated mine is dominated by sulfide minerals; this contrasts, for example, with the abundance of oxide minerals at the Hidden Treasure mine.

Tiny veinlets or stringers of black crystalline scheelite were found in the hanging wall adjacent to the cave. The only source of ophirite was a six-cm wide and one-meter long veinlet, surrounded by a narrow zone of sericite-containing pyrite, with occasional foci of apatite, bournonite, galena, sphalerite, and other unidentified sulfides; rare crystals of fluorite and sulfur are also present in the veinlet. Among the black scheelite crystals are inclusions and pockets of dolomite. Ophirite crystals occur mostly at the interface between the dolomite and scheelite; it appears that late acidic and oxidizing hydrothermal solutions, in the presence of pyrite and calcium-rich hornfels, reacted with dolomite and scheelite to produce crystals of ophirite.

The compositions of veins in the mine vary considerably. The ore zones, which contain sulfides, were considerably larger and follow the limestone bedding planes. Other phases found

in the mine include adularia, aurichalcite, azurite, boulangerite, bournonite, calcite, carbonatecyanotrichite, cerussite, chalcoalumite, chalcopyrite, cyanotrichite, dolomite, hübnerite, hydrozincite, ktenasite, linarite, malachite, marcasite, quartz, ralstonite, schulenbergite, serpierite, siderite, spangolite, tennantite, and tetrahedrite.

The clear evidence of oxidative alteration of the sulfides, most notably pyrite, is indicative of a late-stage mineral-forming environment that is relatively oxidized; however, the extent of the oxidation, and particularly the oxidation states of Fe and Mn (2+ or 3+), was not immediately evident. To determine oxidation states, we released the oxidation state in the optimization study and conducted optical spectroscopic studies, detailed below. The results, presented below, showed all cations to be in their fully oxidized states: Mg^{2+}, Ca^{2+}, Fe^{3+}, Mn^{3+}, Sb^{5+}, and W^{6+}.

PHYSICAL AND OPTICAL PROPERTIES

Crystals of ophirite are tabular on {001} with irregular {100} and {110} bounding forms; individual crystals are up to about 1 mm in maximum dimension (Figs. 1 and 2). The vitreous and transparent crystals are orange-brown, with a pale orange streak. Ophirite is non-fluorescent in long- and short-wave ultraviolet light. It has a Mohs hardness of 2, brittle tenacity, irregular fracture, and no parting or cleavage. The density of ophirite could not be measured because there is insufficient material for direct measurement and the mineral slowly decomposes in Clerici solution; the calculated density is 4.060 g•cm^{-3} based on the empirical formula using single-crystal cell data.

The optical properties of ophirite were determined in white light. Ophirite is biaxial (+), with $\alpha = 1.730(3)$, $\beta = 1.735(3)$, $\gamma = 1.770(3)$. For ophirite, $2V_{meas} = 43(2)°$ by direct conoscopic

measurement using a spindle stage, and $2V_{calc} = 42.1°$. Dispersion is strong, $r > v$. Orientation (incompletely determined) is $Y \wedge \mathbf{b} \approx 9°$, with one optic axis approximately perpendicular to {001}. The pleochroism is X = light orange brown, Y = light orange brown, Z = orange brown; $X < Y << Z$.

OPTICAL SPECTROSCOPY

Optical spectra of ophirite (Fig. 3) were obtained on a 62 μm diameter spot on an approximately 14.2 μm thick, 176 × 88 μm fragment with a prominent (001) face. Spectra were obtained with linearly polarized light oriented parallel to both extinction directions on this face. In this orientation, light was propagating close to one of the optic axes. A custom-built optical micro-spectrometer with a silicon diode-array detector was used.

The spectra in the two extinction directions are similar, showing an absorption tail rising towards the ultraviolet end of the spectrum with an obvious absorption band of moderate intensity superimposed at about 500 nm. Curve fitting indicates that the band is at about 490 nm. The spectra of Mn^{3+} phases commonly occur in the 500 nm region, usually at a slightly longer wavelength, but sometimes at a slightly shorter wavelength.

To further test if this band could be from either Mn^{2+} or Mn^{3+}, the molar absorptivity (ε-value) was calculated from the average MnO content (2.25 wt%), the absorbance determined from the curve fitting (about 0.1) and the density (4.06 gm•cm^{-3}). A Beer's law calculation indicates that the ε-value is about 54, if all of the Mn contributes to this band. This is a value consistent with a spin-allowed absorption from Mn^{3+}, but is inconsistent with the much less-intense spin-forbidden absorptions of Mn^{2+} that may have lower epsilons in this region (for example, epsilon for rhodochrosite is about 0.05 for the absorption bands between 450 and 550

nm). The only other cation likely to contribute to the optical absorption spectrum is iron, which is present at a concentration in the same range as manganese. Because the Fe^{2+} spectrum is expected to occur at 800 nm or longer wavelengths, this oxidation state can be ruled out as the cause of the 500 nm absorption.

Like Mn^{2+}, Fe^{3+} also has spin-forbidden transitions, but when in a tetrahedral site will have greater intensity than when in the more common octahedral sites of low absorption intensity. Two standards of Fe in tetrahedral oxygen coordination have been presented. In the spectrum of γ-$LiAlO_2$, a band at 450 nm with $\varepsilon = 17.2$ is prominent, along with significantly weaker features between 500 and 600 nm (Waychunas and Rossman 1983). In the spectrum of tetrahedral Fe^{3+} in orthoclase (Faye 1969), a pair of bands occur at 417 and 441 nm with epsilon of about 1.5, with a much weaker band at 483 nm. Published data for potential standards for a ferri-heteropolytungstate could not be located for the visible spectral region

Neither of these standards has bands in the 490 nm region that are as intense as those of the ophirite spectrum. Thus, it is likely that, if tetrahedral ferric iron were present in ophirite, its presence could not be confirmed by optical spectroscopic methods. The optical spectrum suggests four observations on Fe and Mn valence state: 1) Fe^{2+} is not present in ophirite, 2) Mn as Mn^{3+} is plausible in ophirite, 3) absorption caused by Mn^{2+} would be too weak to observe in the optical spectrum, and 4) absorption caused by tetrahedral Fe^{3+} would be difficult or impossible to observe in the optical spectrum. These results are consistent with the results of the structural optimization, which indicates that all species are in their fully oxidized states.

RAMAN SPECTROSCOPY

The Raman spectrum of ophirite was collected with a Renishaw M-1000 microRaman

system with a 514.5 nm argon ion laser and a 100× objective that produced a spot of about 1.2 μm diameter with a depolarizer in the beam directly above the sample. Power at the sample was raised from 0.5 mW to 5 mW with no visible sample damage.

The ophirite Raman spectrum in Figure 4 bears close resemblance to the spectra of the other heteropolytungstates, as described by Detusheva et al. (2003). The spectra are dominated by the W=O stretching in the 900-960 cm^{-1} region. The W–O–W bridge vibrations that occur in the 800–500 cm^{-1} region and the W–O vibrations in the 250–200 cm^{-1} region are relatively weak.

CHEMICAL ANALYSIS

Analyses of ophirite (14 on two crystals) were performed at the University of Utah on a Cameca SX-50 electron microprobe with four wavelength-dispersive spectrometers. Analytical conditions were 15 KeV accelerating voltage, 10 nA beam current and a beam diameter of 10 μm. Counting times were 20 seconds for each element. Raw X-ray intensities were corrected for matrix effects with a $\phi\rho(z)$ algorithm (Pouchou and Pichoir 1991).

Because insufficient material was available for a direct determination of H_2O, the amount of water in ophirite was calculated on the basis of 30 total cations (Ca+Mg+Zn+Mn+Fe+Sb+W), charge balance, and 116 O atoms *pfu*, as determined by the crystal structure analysis (see below). The results are presented in Table 1. The empirical formula of ophirite on this basis is $Ca_{1.73}Mg_{3.99}[Zn_{2.02}(Mn^{3+}_{1.82}Sb^{5+}_{0.22})(H_2O)_2(Fe^{3+}_{2.34})(W_{17.99})O_{68}] \cdot 45.95H_2O$. Such a casting of the formula ignores the extensive substitution in the ophirite structure. There is complex substitution among the cation sites in ophirite, which was quantified using optimization methods (Wright et al. 2000); that substitution is discussed subsequently. The ideal formula of ophirite is $Ca_2Mg_4[Zn_2Mn^{3+}_2(H_2O)_2(Fe^{3+}W_9O_{34})_2] \cdot 46H_2O$.

188

189 **X-RAY CRYSTALLOGRAPHY AND STRUCTURE DETERMINATION**

190 Powder and single-crystal X-ray diffraction data for ophirite were obtained on a Rigaku
191 R-Axis Rapid II curved imaging plate microdiffractometer using monochromatized MoKα
192 radiation. The powder data presented in Table 2 for ophirite are in good agreement with those
193 calculated from the structure data. Observed *d* values and intensities were derived by profile
194 fitting using JADE 2010 software.

195 The Rigaku CrystalClear software package was used for reducing X-ray intensity data to
196 structure factors, including corrections for Lorentz and polarization effects and the application of
197 empirical absorption corrections; the structures were solved by direct methods using SIR2004
198 (Burla et al. 2005). The SHELXL-97 software (Sheldrick 2008) was used for the structure
199 refinements, utilizing neutral-atom scattering factors. Hydrogen atoms were located using
200 difference Fourier maps, and were refined using O–H and H–H distance restraints. The
201 occupancy of all non-H cations except Mg was released in order to determine the total electron
202 count at those sites, values used subsequently in the optimization of cation occupancy. Details of
203 the data collections and structure refinements are provided in Table 3, and the atom coordinates
204 and equivalent displacement parameters are in Table 4. Table 5 lists selected interatomic
205 distances. A copy of anisotropic displacement parameters, a table of observed and calculated
206 structure factors, and the CIF file for ophirite are on deposit and available as listed below.[1]

207

[1] Deposit items AM-14-xx1, AM-14-xx2 and AM-14-xx3 give anisotropic displacement parameters, observed and calculated structure factors, and CIF, respectively. Deposit items are available two ways: for paper copies contact the Business Office of the Mineralogical Society of America (see inside front cover of recent issue) for price information. For an electronic copy visit the MSA web site at http://www.minsocam.org, go to the *American Mineralogist* Contents, find the table of contents for the specific volume/issue wanted, and then click on the deposit link there.

DESCRIPTION OF THE STRUCTURE

Ophirite is a bipartite structure that consists of a *structural unit* and an *interstitial unit*, as elucidated by Schindler & Hawthorne (2001). The $\{^{[6]}Zn_2{}^{[6]}Mn^{3+}{}_2(H_2O)_2(^{[4]}Fe^{3+[6]}W^{6+}{}_9O_{34})_2\}^{12-}$ heteropolyanion defines the structural unit, the anionic portion of the structure. The more rigid structural units are linked by the interstitial unit, the cationic portion of the structure, with bonds of lower bond-valence linking Mg and Ca to an O atom of the structural unit and/or interstitial H_2O groups. The interstitial unit in ophirite, $\{[Mg(H_2O)_6]_4[Ca(H_2O)_6]_2 \bullet 10H_2O\}^{12+}$, balances the charge of the structural unit and links the structural units together. The atomic arrangement of ophirite is depicted in Figure 5.

The $\{^{[6]}Zn_2{}^{[6]}Mn^{3+}{}_2(H_2O)_2(^{[4]}Fe^{3+[6]}W^{6+}{}_9O_{34})_2\}^{12-}$ structural unit

The structural unit in ophirite consists of the $\{^{[6]}Zn_2{}^{[6]}Mn^{3+}{}_2(H_2O)_2(^{[4]}Fe^{3+[6]}W^{6+}{}_9O_{34})_2\}^{12-}$ polyanion (Fig. 6). That polyanion is formed of two $(^{[4]}Fe^{3+[6]}W^{6+}{}_9O_{34})$ groups (Fig. 7), with an intervening $Zn_2Mn^{3+}{}_2(H_2O)_2$ edge-sharing octahedral layer formed of two $Mn^{3+}O_6$ and two $ZnO_5(H_2O)_1$ octahedra that share oxygen atoms with the $(^{[4]}Fe^{3+[6]}W^{6+}{}_9O_{34})$ groups. Although ophirite is the first known mineral to contain the $(^{[4]}Fe^{3+[6]}W^{6+}{}_9O_{34})$ group, the $\{XM_9O_{34}\}$ heteropolyanion is well-known in synthetic compounds.

Keggin (1934) was the first to solve the atomic arrangement of the heteropolyanionic $(XM_{12}O_{40})$ group, using X-ray diffraction methods. Now known as the Keggin heteropolyanion, the heteropoly acid is formed of twelve M–O octahedra surrounding a central tetrahedral cation, X; the most common M cations are Mo and W. The Keggin heteropolyanion is also known to spawn defect structures in which one or more of the octahedra are removed from the $(XM_{12}O_{40})$ Keggin anion, such as $(XM_{11}O_{39})$, a defect structure in which one octahedron is absent from the

Keggin anion, and the (XM_9O_{34}) group, a defect structure in which three octahedra are absent from the Keggin anion. Such heteropolyanions are known as "lacunary Keggin structures" to note the defect structures caused by the missing octahedra; the (XM_9O_{34}) group is also known as a "tri-lacunary" because of the deficiency of three octahedra. A rich literature exists on the chemistry and structure of lacunary Keggin anions.

The heteropolytungstate ($^{[4]}Fe^{3+[6]}W^{6+}{}_9O_{34}$) in ophirite is a tri-lacunary Keggin anion of the α-B-(XM_9O_{34}) type, and it forms the foundation of the structural unit in ophirite. In ophirite, two of the $\{XM_9O_{34}\}$ tri-lacunary Keggin anions ($X = Fe^{3+}$, $M = W^{6+}$; Fig. 7) create a "sandwich" structure with four intervening coplanar edge-sharing octahedra ($2 \times [(Mn^{3+}O_6) + (ZnO_5(H_2O)_1)]$) between opposing $\{Fe^{3+}W_9O_{34}\}$ groups, yielding the structural unit of $\{^{[6]}Zn_2{}^{[6]}Mn^{3+}{}_2(H_2O)_2(^{[4]}Fe^{3+[6]}W^{6+}{}_9O_{34})_2\}^{12-}$ depicted in Figure 6. Although ophirite is the first example of the tri-lacunary polyanion in minerals, the sandwich structure with four intervening octahedra between two tri-lacunary Keggin anions is well-known in synthetic compounds (*e.g.*, Li et al. 2009, Limanski et al. 2002, Bosing et al. 1997 and references therein).

The $\{[Mg(H_2O)_6]_4[Ca(H_2O)_6]_2 \cdot 10H_2O\}^{12+}$ interstitial unit

As noted by Schindler and Hawthorne (2001), the charge of the anionic structural units is balanced by the cationic interstitial unit. The interstitial unit in the structure of ophirite is formed of two distinct $Mg(H_2O)_6$ octahedra and a $Ca(H_2O)_6O_1$ polyhedron, as well as five isolated water molecules. Note that the oxygen atom of the $Ca(H_2O)_6O_1$ polyhedron is shared with one of the W octahedra of the structural unit, whereas the remainder of the linkage between the structural unit and the interstitial unit is attained through hydrogen bonding. The complete interstitial unit (not including the oxygen atom shared with the structural unit) has a composition of

254 $\{[Mg(H_2O)_6]_4[Ca(H_2O)_6]_2 \bullet 10H_2O\}^{12+}$, balancing the charge of the structural unit with its
255 extensive cation substitutions, and yielding the simplified structural formula
256 $\{[Mg(H_2O)_6]_4[Ca(H_2O)_6]_2 \bullet 10H_2O\}^{12+}\{Zn_2Mn^{3+}{}_2(H_2O)_2(Fe^{3+}{}_2W_{18}O_{68})\}^{12-}$ for ophirite.
257

258 **Cation substitution**

259 The extensive substitution among the cations and cation sites in ophirite was elucidated
260 using the program OccQP (Wright et al. 2001), which uses a constrained least-squares
261 formulation to optimize occupancy assignments based upon site scattering, chemical
262 composition, charge balance, bond valence and cation-anion bond lengths. The results of the
263 optimization are provided in Table 6. Those results demonstrate the extensive cation solution in
264 both the structural unit and interstitial unit, which yields the charge balance in ophirite. The
265 method was also used to determine the "best-fit" valence state for Fe and Mn, as the program
266 was free to vary the valence state of these cations during the minimization process; as expected,
267 all Fe was found to be Fe^{3+}, and the Mn results are in accord with the optical spectroscopic
268 results that are consistent with all Mn as Mn^{3+}.

269 The simplified structural formula for ophirite can be written:
270 $\{[Mg(H_2O)_6]_4[Ca(H_2O)_6]_2 \bullet 10H_2O\}\ \{Zn_2Mn^{3+}{}_2\,(H_2O)_2\,(Fe^{3+}{}_2W_{18}O_{68})\}$. Given the results of the
271 optimization, the parallel detailed structural formula for ophirite can be written as:
272 $\{[(Mg,Mn)(H_2O_6)]_4\,[(Ca,Mg,Zn)(H_2O)_6]_2 \bullet 10H_2O\}\,\{(Zn,Fe^{3+},Ca,Sb^{5+})_{\Sigma 2.00}$
273 $(Mn^{3+},Sb^{5+},Fe^{3+},W)_{\Sigma 2.00}\,(H_2O)_2\,[(Fe^{3+},Sb^{5+},Ca,Mg)_{\Sigma 2.00}\,(W^{6+},Mn^{3+})_{\Sigma 18.00}O_{68}]\}$. The quantification
274 of the substitutions is given in Table 6.
275

276 **IMPLICATIONS**

Many complex heteropoly anions have been synthesized, and they have long been used in industry and as catalysts in chemical processes. The most widely known heteropoly anion is the Keggin anion, for which a large body of literature exists. Until now, minerals containing the Keggin anion were not known to occur. Ophirite is the first known mineral to contain a lacunary defect derivative of the Keggin anion and its description introduces that polyanion and its associated structural groups to the mineralogical literature. The occurrence of ophirite demonstrates the natural conditions under which Keggin anions can form, and suggests that other members of this class of compounds occur naturally.

ACKNOWLEDGEMENTS

We are grateful to Leo Ault, mine owner, who allowed access to the Ophir Hill Consolidated mine for collecting. The manuscript was improved by reviews by Joel Grice and Stefan Graeser, and Editors Fernando Colombo and Ross John Angel both also provided helpful comments. This study was funded, in part, by the John Jago Trelawney Endowment to the Mineral Sciences Department of the Natural History Museum of Los Angeles County and by National Science Foundation grants NSF-MRI 1039436 to JMH and EAR-0947956 to GRR.

295

296 **REFERENCES**

297

298 Barats, D., Leitus, G., Popovitz-Biro, R., Shimon, L.J.W. and Neumann, R. (2008) A stable
299 "End-On" iron(III)-hydroperoxo complex in water derived from a multi-iron(II)
300 polyoxometalate and molecular oxygen. Angewandte Chemie International Edition 2008, 47,
301 9908–9912.
302 Bösing, M., Loose, I., Pohlmann, H. and Krebs, B. (1997) New strategies for the generation of
303 large heteropolymetalate clusters: The β-B-SbW_9 fragment as a multifunctional unit.
304 Chemistry: A European Journal, 3, 1232–1237.
305 Burla, M.C., Caliandro, R., Camalli, M., Carrozzini, B., Cascarano, G.L., De Caro, L.,
306 Giacovazzo, C., Polidori, G. and Spagna, R. (2005) SIR2004: an improved tool for crystal
307 structure determination and refinement. Journal of Applied Crystallography, 38, 381–388.
308 Detusheva, L.G., Kuznetsova, L.I., Dovlitova, L.S., and Likholobov, V.A. (2003) Study of the
309 equilibrium of formation of arsenic(III) lacunar heteropolytungstates by Raman
310 spectroscopy. Russian Chemical Bulletin, International Edition, 52, 370–374.
311 Faye, G.H. (1969) The optical absorption spectrum of tetrahedrally bonded Fe^{3+} in orthoclase.
312 Canadian Mineralogist, 10, 112–117.
313 Keggin, J.F. (1934) The Structure and Formula of 12-Phosphotungstic Acid. Proceedings of the
314 Royal Society, A, 144, 75–100.
315 Li, B., Yan, Y., Li, F., Xu, L., Bi, L., and Wua, L. (2009) Synthesis, crystal structure, and
316 properties of two sandwich-type tungstovanadates. Inorganica Chimica Acta, 362, 2796–
317 2801.

Limanski, E.M., Piepenbrink, M., Droste, E., Burgmeister, K. and Krebs, B. (2002) Syntheses and X-ray characterization of novel $[M_4(H_2O)_2(XW_9O_{34})_2]^{n-}$ ($M=Cu^{II}$, $X=Cu^{II}$; and $M=Fe^{III}$, $X=Fe^{III}$ polyoxotungstates. Journal of Cluster Science, 13, 369–379.

Marty, J. and Wise, W.S. (2008) Minerals from the Hidden Treasure and other mines in the Ophir District, Tooele County, Utah. Rocks and Minerals, 83, 52–62.

Pouchou, J.-L. and Pichoir, F. (1991) Quantitative analysis of homogeneous or stratified microvolumes applying the model "PAP." In K.F.J. Heinrich and D.E. Newbury, Eds. Electron probe quantitation, p. 3 l–75. Plenum Press, New York.

Schindler, M., and Hawthorne, F.C. (2001) A bond-valence approach to the structure, chemistry, and paragenesis of hydroxyl-hydrated oxysalt minerals. I. Theory. The Canadian Mineralogist, 39, 1225-1242.

Sheldrick, G.M. (2008) A short history of SHELX. Acta Crystallographica, A64, 112–122.

Waychunas, G.A., and Rossman, G.R. (1983) Spectroscopic standard for tetrahedrally coordinated ferric iron: γ-$LiAlO_2$: Fe^{3+}. Physics and Chemistry of Minerals, 9, 212–215.

Wright, S.E., Foley, J.A. and Hughes, J.M. (2000) Optimization of site occupancies in minerals using quadratic programming. American Mineralogist, 85, 524–531.

335 **TABLE 1**. Analytical results for ophirite.
336
337

Const.	Wt%	S.D. (metal)	Ideal Wt%†	Standard
CaO	1.68	0.61	1.94	diopside
MgO	2.79	0.09	2.78	diopside
ZnO	2.86	0.36	2.81	Zn Metal
Mn_2O_3	2.50	0.22	2.73	rhodonite
Fe_2O_3	3.25	0.20	2.76	hematite
Sb_2O_5	0.61	0.13	–	GaSb (syn)
WO_3	71.94	1.01	72.06	W metal
H_2O	15.24*		14.92	
Total	100.87		100.00	

338 * Based on structure
339 † Calculated using $Ca_2Mg_4[Zn_2Mn^{3+}{}_2(H_2O)_2(Fe^{3+}W_9O_{34})_2]\bullet 46H_2O$.
340
341
342
343

344 **TABLE 2.** Powder X-ray diffraction data for ophirite.

I_{obs}	d_{obs}	d_{calc}	I_{calc}	$h\,k\,l$	I_{obs}	d_{obs}	d_{calc}	I_{calc}	$h\,k\,l$	I_{obs}	d_{obs}	d_{calc}	I_{calc}	$h\,k\,l$
38	16.72	16.5383	45	0 0 1			2.6365	5	4 0 1			1.7298	1	1 $\bar{4}$ 5
91	11.33	11.2739	100	0 1 1	33	2.594	2.5916	3	4 1 3			1.7283	1	2 ·3·10
		11.2164	19	0 1 0			2.5822	6	3 4 5	14	1.722	1.7241	4	$\bar{1}$ ·2·10
100	10.69	10.8185	52	1 0 0			2.5690	3	$\bar{1}$ 4 1			1.7208	1	4 6 8
		10.2594	51	1 1 0	7	2.506	2.5087	6	$\bar{1}$ 4 4			1.7140	2	4 0 7
		9.8552	8	1 1 1	17	2.382	2.3829	6	$\bar{4}$ $\bar{1}$ 4			1.6842	2	$\bar{4}$ $\bar{1}$ 8
		9.3972	15	$\bar{1}$ 0 1			2.3562	5	4 0 3	4	1.685	1.6811	2	$\bar{2}$ $\bar{7}$ 1
55	8.27	8.2692	56	0 0 2	5	2.239	2.2340	2	$\bar{1}$ 4 6			1.6580	1	7 5 1
		8.0735	15	0$\bar{1}$ 1			2.2302	3	$\bar{2}$ 0 7			1.6561	1	$\bar{2}$ 6 3
12	6.04	5.9994	4	1 2 2	12	2.176	2.1824	3	1 $\bar{4}$ 2			1.6545	1	3·3·10
		5.9786	5	0 2 1			2.1655	6	0$\bar{1}$ 7	11	1.651	1.6501	1	$\bar{2}$ ·2·10
33	5.44	5.4408	10	$\bar{2}$ $\bar{1}$ 1	6	2.117	2.1247	2	$\bar{1}$ 2 8			1.6487	3	7 5 3
7	5.30	5.2750	9	2 2 1			2.1108	2	$\bar{4}$ 2 0			1.6446	2	$\bar{6}$ $\bar{5}$ 3
		5.2646	9	$\bar{2}$ 0 1			2.0797	2	4 6 3			1.6186	2	2 8 5
7	4.825	4.8267	6	0 $\bar{2}$ 1	6	2.067	2.0692	1	$\bar{3}$ 3 5			1.6147	2	0 $\bar{5}$ 5
16	4.519	4.4889	6	$\bar{1}$ 2 1			2.0673	1	0 0 8			1.6115	1	5 7 7
18	4.335	4.3412	7	1 3 2			2.0635	1	1 6 1	20	1.612	1.6105	1	$\bar{3}$ $\bar{4}$ 7
		4.2964	6	$\bar{1}$ $\bar{2}$ 2			2.0012	1	$\bar{4}$ $\bar{1}$ 6			1.6023	1	0 7 0
		4.1359	9	1 2 4	6	1.992	1.9967	1	3 3 8			1.6008	2	1 $\bar{4}$ 6
27	4.119	4.1133	2	1 3 0			1.9892	1	$\bar{1}$ $\bar{3}$ 6			1.5998	3	3 $\bar{1}$ 8
		4.1007	3	2 3 2			1.9230	1	0 $\bar{3}$ 6	10	1.588	1.5837	5	$\bar{3}$ $\bar{5}$ 6
		4.0909	3	$\bar{2}$ 1 2			1.9217	1	6 4 3			1.5608	3	$\bar{1}$ ·3·11
		3.6208	7	3 1 2			1.9133	2	$\bar{3}$ $\bar{4}$ 5	20	1.554	1.5589	2	$\bar{5}$ 2 7
15	3.588	3.6066	4	$\bar{2}$ $\bar{3}$ 1	33	1.916	1.9119	1	6 1 0			1.5472	3	7 1 3
		3.5484	6	$\bar{1}$ 2 4			1.9089	3	3 0 7			1.5368	3	6 4 8
13	3.464	3.4673	12	3 0 1			1.9058	1	$\bar{1}$ 2 9			1.5021	3	$\bar{7}$ $\bar{5}$ 3
3	3.319	3.3077	7	0 0 5			1.9047	1	3 $\bar{1}$ 6	11	1.498	1.5000	2	$\bar{4}$ $\bar{2}$ 9
30	3.190	3.1993	15	$\bar{1}$ 3 3			1.8989	4	$\bar{4}$ 3 2			1.4952	2	2·7·10
		3.0196	6	3 3 4			1.8596	3	6 5 3	10	1.466	1.4680	2	4 $\bar{4}$ 3
75	2.992	2.9947	16	3 4 1	18	1.856	1.8530	2	6 1 2			1.4673	3	6 8 6
		2.9462	9	$\bar{1}$ $\bar{1}$ 5			1.8513	3	$\bar{4}$ 3 4			1.4483	1	2·3·12
16	2.913	2.9150	7	3 0 3			1.8071	4	$\bar{5}$ 2 2	3	1.443	1.4429	1	$\bar{2}$ 7 2
		2.9107	17	0$\bar{1}$ 5			1.8047	1	$\bar{2}$ 2 9			1.4423	2	6 8 0
		2.7645	8	4 1 2			1.8039	1	$\bar{5}$ 1 5			1.4418	1	7 1 5
55	2.760	2.7564	21	0 0 6	15	1.799	1.8009	1	0 6 7					
		2.7522	11	$\bar{1}$ 3 5			1.7943	1	$\bar{1}$ $\bar{3}$ 7					
		2.7102	9	$\bar{3}$ $\bar{4}$ 1			1.7933	1	2 7 6					
							1.7916	1	$\bar{1}$ 6 5					

Only calculated lines with intensities greater than 7 are listed unless they correspond to observed lines. Mismatches in intensities between observed and calculated lines are due to the large number of lines of relatively low intensity that are not listed.

350 **TABLE 3.** Sample and crystal data for ophirite.

351

Formula weight	5726.57	
Temperature	293(2) K	
Wavelength	0.71075 Å	
Crystal size	0.040 x 0.090 x 0.100 mm	
Crystal system	Triclinic	
Space group	$P\bar{1}$	
Unit cell dimensions	a = 11.9860(2) Å	α = 69.690(5)°
	b = 13.2073(2) Å	β = 85.364(6)°
	c = 17.6891(12) Å	γ = 64.875(5)°
Volume	2370.35(18) Å^3	
Absorption coefficient	22.543 mm^{-1}	
F(000)	2579	
Theta range	3.06 to 27.46°	
Index ranges	$-15 \leq h \leq 15$, $-17 \leq k \leq 17$, $-22 \leq \ell \leq 22$	
Reflections collected	76,304	
Independent reflections	10,834 [R_{int} = 0.0578]	
Completeness	99.8%	
Max. and min. transmission	0.4658 and 0.2114	
Structure solution	direct methods	
Structure solution program	SHELXS-97 (Sheldrick, 2008)	
Refinement method	Full-matrix least-squares on F^2	
Refinement program	SHELXL-97 (Sheldrick, 2008)	
Function minimized	$\Sigma\, w(F_o^2 - F_c^2)^2$	
Data / restraints / parameters	10834 / 72 / 802	
Goodness-of-fit on F^2	1.034	
Δ/σ_{max}	0.002	
Final R indices	9,230 data;	
	$I > 2\sigma(I)$	R_1 = 0.0298, wR_2 = 0.0671
	all data	R_1 = 0.0386, wR_2 = 0.0704
Weighting scheme	$w = 1/[\sigma^2(F_o^2)+(0.0338P)^2+11.0210P]$ where $P = (F_o^2+2F_c^2)/3$	
Largest diff. peak and hole	2.059 and -1.388 e·Å^{-3}	

353
354

355

356 **TABLE 4.** Atomic coordinates and equivalent isotropic displacement parameter for atoms in

357 ophirite.

	x/*a*	*y*/*b*	*z*/*c*	U_{eq}*
M1	0.89860(8)	0.63418(7)	0.32977(5)	0.01612(17)
M2	0.97962(8)	0.61798(7)	0.51246(5)	0.02115(18)
M3	0.74884(9)	0.56532(8)	0.49729(6)	0.0269(2)
M4	0.2029(2)	0.0955(2)	0.15709(14)	0.0242(5)
M5	0.5557(3)	0.2693(2)	0.14317(18)	0.0368(6)
M6	0.72573(18)	0.12204(16)	0.47144(11)	0.0345(4)
W1	0.62958(3)	0.59597(3)	0.305958(18)	0.02324(7)
W2	0.68205(3)	0.79959(3)	0.153583(17)	0.02192(7)
W3	0.59807(3)	0.84097(3)	0.329077(18)	0.02213(7)
W4	0.14645(3)	0.70577(3)	0.33653(17)	0.02102(7)
W5	0.95150(3)	0.86633(3)	0.173366(17)	0.02129(7)
W6	0.87027(3)	0.89918(2)	0.350128(17)	0.02192(7)
W7	0.00624(3)	0.58314(3)	0.144552(17)	0.02216(7)
W8	0.94939(3)	0.37895(3)	0.294331(17)	0.02156(7)
W9	0.19665(3)	0.42058(3)	0.309721(17)	0.02161(7)
O1	0.7321(4)	0.7060(4)	0.2866(3)	0.0210(10)
O2	0.9553(4)	0.7555(4)	0.3003(3)	0.0209(10)
O3	0.9977(4)	0.5250(4)	0.2781(3)	0.0197(10)
O4	0.9122(4)	0.5581(4)	0.4444(3)	0.0218(10)
O5	0.8794(5)	0.7852(4)	0.4474(3)	0.0246(11)
O6	0.0426(5)	0.6511(4)	0.5971(3)	0.0250(11)
O7	0.1226(5)	0.6184(4)	0.4410(3)	0.0247(11)
O8	0.1641(5)	0.3971(4)	0.4185(3)	0.0253(11)
O9	0.6865(5)	0.5239(5)	0.4098(3)	0.0289(12)
O10	0.6509(5)	0.7451(5)	0.4316(3)	0.0286(12)
O11	0.5286(5)	0.5364(5)	0.2978(3)	0.0303(12)
O12	0.5141(5)	0.7428(5)	0.3179(3)	0.0291(12)
O13	0.7827(5)	0.4838(5)	0.2756(3)	0.0275(11)
O14	0.6050(5)	0.6960(4)	0.1843(3)	0.0266(11)
O15	0.6168(6)	0.8799(5)	0.0549(3)	0.0340(13)
O16	0.5731(5)	0.9049(4)	0.2047(3)	0.0247(11)
O17	0.8326(5)	0.6755(4)	0.1391(3)	0.0252(11)

O18	0.7967(5)	0.8715(4)	0.1578(3)	0.0270(11)
O19	0.4642(5)	0.9581(5)	0.3392(4)	0.0382(14)
O20	0.7123(5)	0.9098(5)	0.3169(3)	0.0284(12)
O21	0.2886(5)	0.7037(5)	0.3521(3)	0.0315(12)
O22	0.1959(5)	0.5725(4)	0.3038(3)	0.0250(11)
O23	0.1154(5)	0.8141(5)	0.2224(3)	0.0272(11)
O24	0.0454(5)	0.8539(4)	0.3621(3)	0.0240(11)
O25	0.9623(6)	0.9683(5)	0.0834(3)	0.0348(13)
O26	0.0207(5)	0.7209(4)	0.1488(3)	0.0244(11)
O27	0.8823(5)	0.9761(4)	0.2318(3)	0.0254(11)
O28	0.8154(5)	0.0273(5)	0.3747(3)	0.0314(12)
O29	0.0296(6)	0.5985(5)	0.0440(3)	0.0348(13)
O30	0.1752(5)	0.4874(4)	0.1891(3)	0.0253(11)
O31	0.9749(5)	0.4413(4)	0.1759(3)	0.0273(12)
O32	0.9489(5)	0.2500(5)	0.2893(3)	0.0304(12)
O33	0.1392(5)	0.3097(4)	0.3052(3)	0.0255(11)
O34	0.3551(5)	0.3334(5)	0.3164(3)	0.0335(13)
O35	0.3672(5)	0.0920(5)	0.1080(3)	0.0344(13)
H35A	0.429(6)	0.027(5)	0.139(4)	0.041
H35B	0.367(8)	0.095(7)	0.058(2)	0.041
O36	0.2537(5)	0.1214(5)	0.2560(4)	0.0366(14)
H36A	0.332(4)	0.080(6)	0.277(5)	0.044
H36B	0.219(6)	0.188(5)	0.269(5)	0.044
O37	0.2893(6)	0.9127(5)	0.2153(4)	0.0422(15)
H37A	0.220(4)	-0.081(9)	0.238(5)	0.051
H37B	0.351(5)	-0.116(8)	0.253(4)	0.051
O38	0.0402(6)	0.0990(6)	0.2066(4)	0.0404(15)
H38A	0.002(7)	0.055(7)	0.203(5)	0.048
H38B	0.091(7)	0.054(7)	0.252(4)	0.048
O39	0.1247(6)	0.2796(5)	0.1008(4)	0.0387(14)
H39A	0.076(7)	0.301(7)	0.060(4)	0.046
H39B	0.101(8)	0.323(7)	0.132(4)	0.046
O40	0.1533(6)	0.0698(7)	0.0582(4)	0.0485(17)
H40A	0.213(5)	0.014(7)	0.043(6)	0.058
H40B	0.079(4)	0.088(8)	0.040(6)	0.058
O41	0.6199(7)	0.1202(6)	0.1149(4)	0.0518(18)
H41A	0.635(9)	0.046(4)	0.146(5)	0.062
H41B	0.551(6)	0.148(7)	0.080(5)	0.062

O42	0.4899(8)	0.4193(6)	0.1739(5)	0.060(2)
H42A	0.525(10)	0.465(9)	0.140(4)	0.072
H42B	0.494(11)	0.425(10)	0.223(3)	0.072
O43	0.5905(7)	0.3576(6)	0.0292(4)	0.0503(17)
H43A	0.534(6)	0.372(9)	-0.010(4)	0.06
H43B	0.665(4)	0.318(9)	0.012(5)	0.06
O44	0.5380(8)	0.1689(6)	0.2588(4)	0.059(2)
H44A	0.489(8)	0.187(8)	0.298(4)	0.07
H44B	0.595(7)	0.093(4)	0.280(5)	0.07
O45	0.3699(8)	0.3200(8)	0.1117(6)	0.070(2)
H45A	0.345(11)	0.261(8)	0.139(6)	0.084
H45B	0.402(11)	0.299(10)	0.067(5)	0.084
O46	0.7354(6)	0.2284(6)	0.1832(4)	0.0468(16)
H46A	0.771(7)	0.279(6)	0.158(6)	0.056
H46B	0.800(6)	0.155(4)	0.197(6)	0.056
O47	0.8161(9)	0.0425(8)	0.6050(5)	0.078(3)
H47A	0.861(8)	0.076(10)	0.616(8)	0.093
H47B	0.736(4)	0.088(10)	0.608(9)	0.093
O48	0.5116(8)	0.1655(8)	0.4577(5)	0.064(2)
H48A	0.501(11)	0.102(7)	0.455(6)	0.077
H48B	0.495(11)	0.167(9)	0.508(3)	0.077
O49	0.6677(7)	0.2764(6)	0.3417(4)	0.0520(18)
H49A	0.703(8)	0.251(7)	0.301(4)	0.062
H49B	0.614(8)	0.353(4)	0.320(5)	0.062
O50	0.0769(7)	0.8691(7)	0.5375(5)	0.0561(18)
H50A	0.082(9)	0.809(7)	0.523(7)	0.067
H50B	0.002(5)	0.900(8)	0.555(7)	0.067
O51	0.6507(7)	0.3100(6)	0.4984(4)	0.0539(18)
H51A	0.591(7)	0.384(4)	0.479(5)	0.065
H51B	0.634(9)	0.272(7)	0.548(3)	0.065
O52	0.7192(8)	0.9252(6)	0.5346(5)	0.066(2)
H52A	0.658(7)	0.997(4)	0.514(7)	0.079
H52B	0.702(10)	0.872(6)	0.524(7)	0.079
O53	0.4133(7)	0.4275(7)	0.9084(5)	0.0589(19)
H53A	0.448(8)	0.358(6)	0.953(4)	0.071
H53B	0.330(4)	0.457(8)	0.920(6)	0.071
O54	0.1818(7)	0.5998(8)	0.9065(5)	0.062(2)
H54A	0.144(9)	0.602(10)	0.953(4)	0.074

H54B	0.148(9)	0.567(10)	0.882(5)	0.074
O55	0.6599(8)	0.3241(9)	0.8424(6)	0.079(3)
H55A	0.672(10)	0.371(10)	0.866(8)	0.095
H55B	0.738(5)	0.285(10)	0.828(8)	0.095
O56	0.8373(9)	0.2245(8)	0.0022(6)	0.078(3)
H56A	0.867(12)	0.226(9)	-0.046(4)	0.094
H56B	0.864(12)	0.148(4)	0.035(5)	0.094
O57	0.6333(8)	0.1289(7)	0.9588(5)	0.060(2)
H57A	0.646(11)	0.115(9)	1.011(2)	0.072
H57B	0.658(10)	0.184(8)	0.928(5)	0.072
O58	0.5965(6)	0.5614(6)	0.5611(4)	0.0407(15)
H58A	0.518(4)	0.616(6)	0.548(5)	0.049
H58B	0.601(7)	0.515(6)	0.612(3)	0.049

*U_{eq} is defined as one third of the trace of the orthogonalized U_{ij} tensor.

TABLE 5. Selected bond distances for atoms in ophirite.

M1–			M2–		M3–	
O2	1.894(5)		O5	1.963(5)	O10	2.074(5)
O1	1.898(5)		O6	1.979(5)	O58	2.079(6)
O3	1.900(5)		O4	2.010(5)	O4	2.079(5)
O4	1.911(5)		O4’	2.022(5)	O9	2.091(5)
Mean	1.901		O7	2.047(5)	O7	2.171(5)
			O8	2.069(5)	O8	2.181(5)
			Mean	2.015	Mean	2.113
M4–			M5–		M6–	
O38	2.061(6)		O41	2.014(7)	O47	2.363(8)
O40	2.069(6)		O42	2.047(7)	O28	2.386(6)
O37	2.069(6)		O43	2.059(7)	O49	2.390(7)
O35	2.076(6)		O44	2.067(7)	O48	2.393(9)
O36	2.076(6)		O45	2.095(9)	O50	2.407(8)
O39	2.079(6)		O46	2.104(7)	O51	2.461(7)
Mean	2.072		Mean	2.064	O52	2.480(8)
					Mean	2.411
W1–			W2–		W3–	
O11	1.739(5)		O15	1.736(5)	O19	1.743(5)
O9	1.785(5)		O14	1.870(5)	O10	1.790(5)
O12	1.918(5)		O16	1.897(5)	O20	1.903(5)
O13	1.983(5)		O17	1.927(5)	O12	2.013(5)
O14	2.064(5)		O18	1.992(5)	O16	2.061(5)
O1	2.200(5)		O1	2.236(5)	O1	2.151(5)
Mean	1.948		Mean	1.943	Mean	1.944
W4–			W5–		W6–	
O21	1.735(6)		O25	1.729(5)	O28	1.734(5)
O7	1.882(5)		O18	1.867(5)	O5	1.825(5)
O22	1.884(5)		O27	1.933(5)	O24	1.930(5)
O23	1.982(5)		O26	1.933(5)	O20	1.961(5)
O24	2.001(5)		O23	1.949(5)	O27	2.008(5)
O2	2.182(5)		O2	2.206(5)	O2	2.188(5)
Mean	1.944		Mean	1.936	Mean	1.941
W7–			W8–		W9–	
O29	1.732(5)		O32	1.739(5)	O34	1.741(5)
O17	1.903(5)		O6	1.824(5)	O8	1.876(5)
O26	1.926(5)		O13	1.860(5)	O33	1.890(5)

O30	1.927(5)	O31	2.018(5)	O22	1.968(5)
O31	1.950(5)	O33	2.057(5)	O30	1.997(5)
O3	2.225(4)	O3	2.162(5)	O3	2.188(5)
Mean	1.944	Mean	1.943	Mean	1.943

421 **TABLE 6**. Site occupants for cation sites in ophirite.

422

Cation Site	Site Occupants
M1	$Fe^{3+}_{0.80}Sb^{5+}_{0.11}Ca_{0.07}Mg_{0.02}$
M2	$Mn^{3+}_{0.71}Sb^{5+}_{0.16}Fe^{3+}_{0.12}W_{0.01}$
M3	$Zn_{0.58}Fe^{3+}_{0.34}Ca_{0.07}Sb^{5+}_{0.01}$
M4	$Mg_{0.99}Mn^{3+}_{0.01}$
M5	$Mg_{0.99}Mn^{3+}_{0.01}$
M6	$Ca_{0.73}Mg_{0.25}Zn_{0.02}$
W1	$W_{0.96}Mn^{3+}_{0.04}$
W2	$W_{0.96}Mn^{3+}_{0.04}$
W3	$W_{0.96}Mn^{3+}_{0.04}$
W4	$W_{0.96}Mn^{3+}_{0.04}$
W5	$W_{0.98}Mn^{3+}_{0.02}$
W6	$W_{0.97}Mn^{3+}_{0.03}$
W7	$W_{0.98}Mn^{3+}_{0.02}$
W8	$W_{0.98}Mn^{3+}_{0.02}$
W9	$W_{0.97}Mn^{3+}_{0.03}$

423
424
425
426

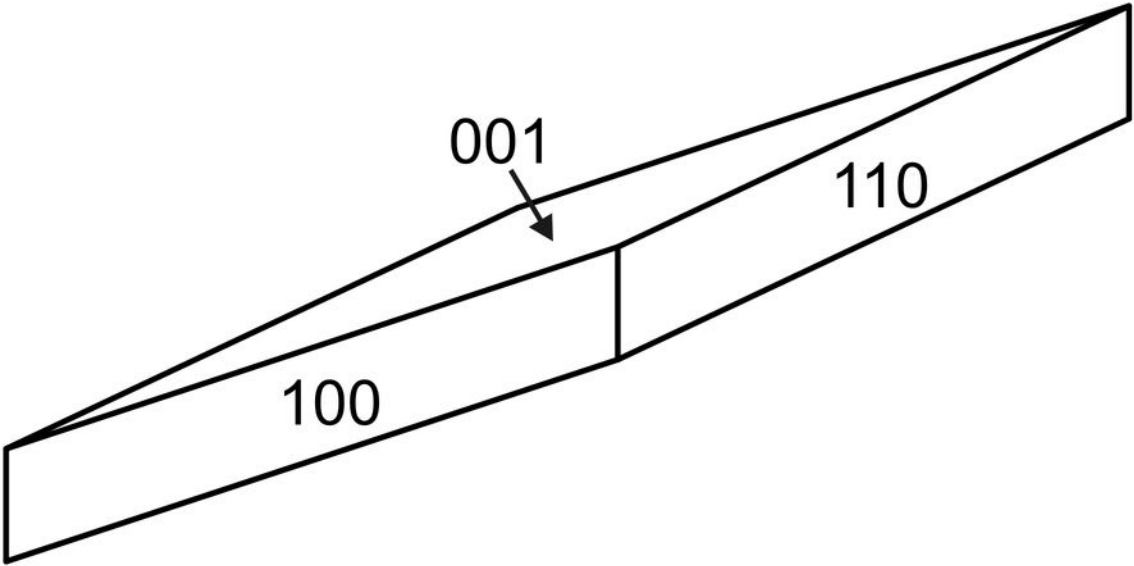
001
110
100

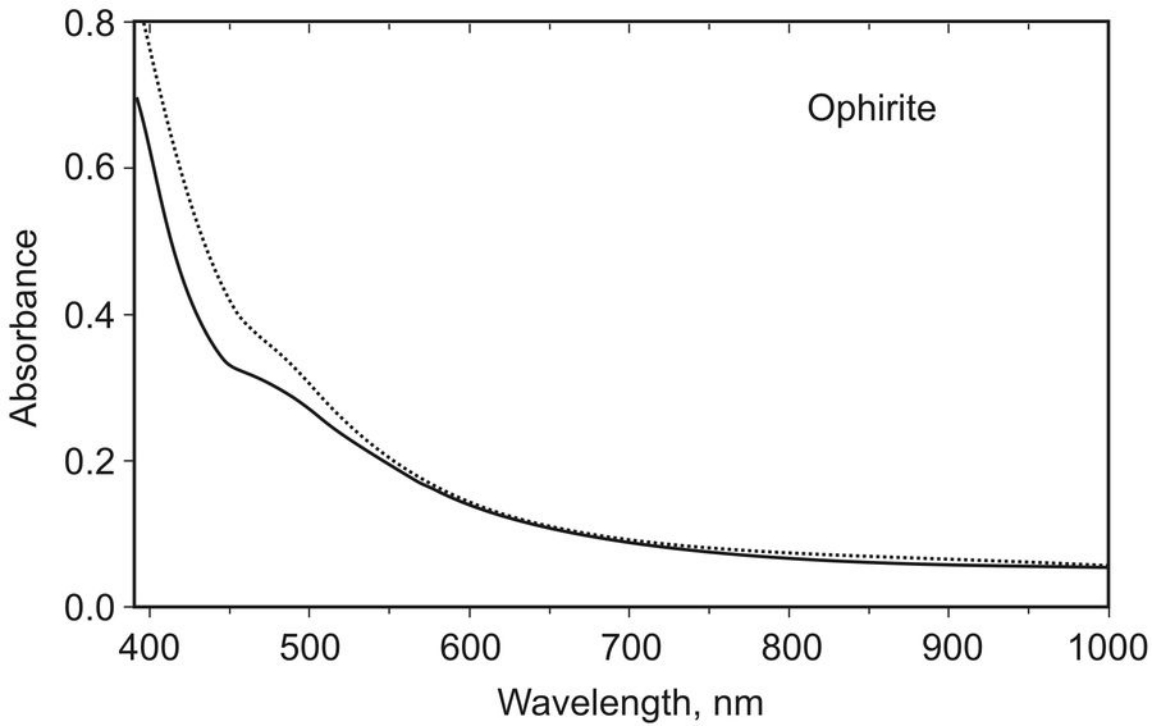
Ophirite
Absorbance
0.0
0.2
0.4
0.6
0.8
400
500
600
700
800
900
1000
Wavelength, nm

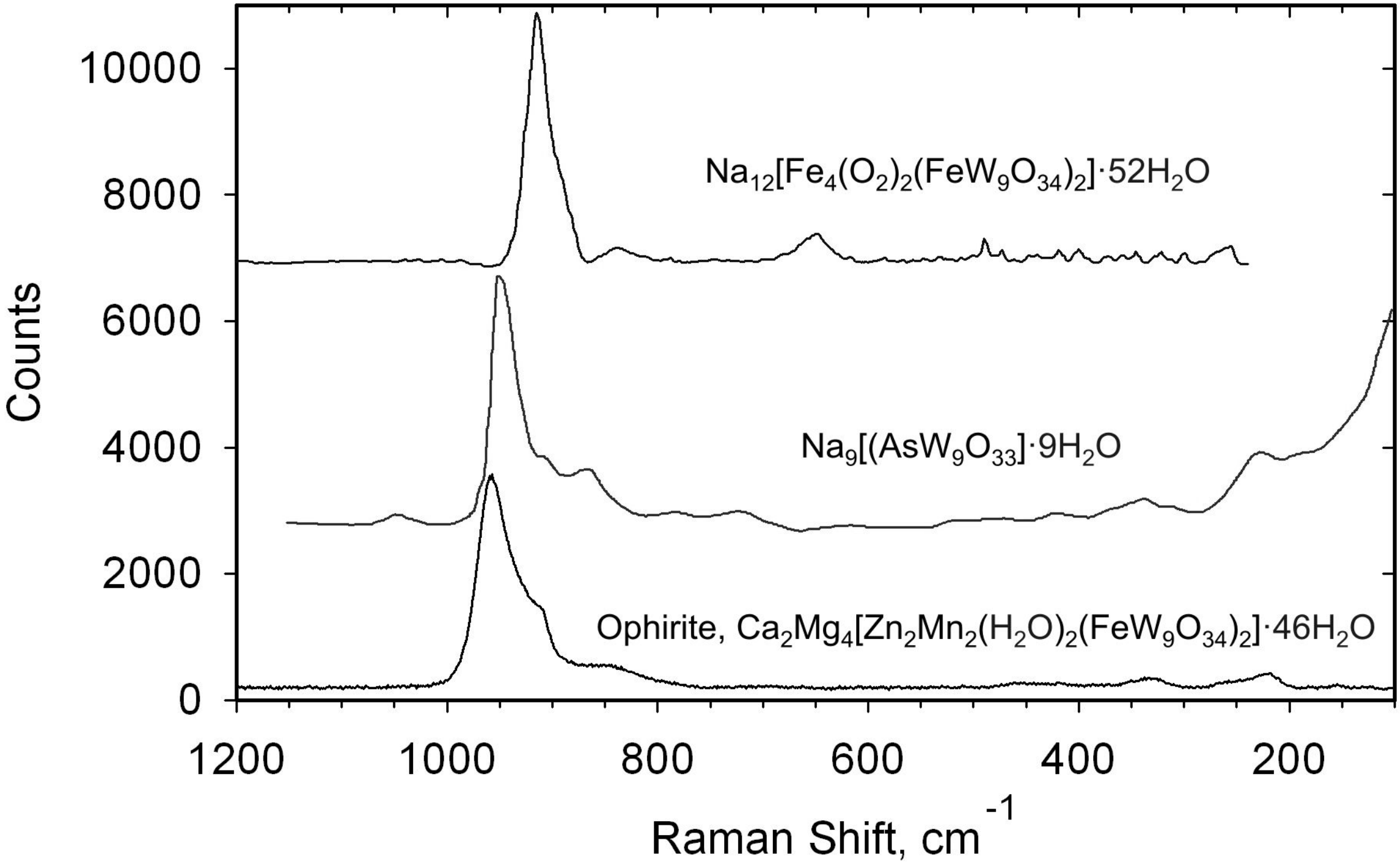
10000
8000
6000
4000
2000
0
Counts
1200
1000
800
600
400
200
Raman Shift, cm-1
Na12[Fe4(O2)2(FeW9O34)2]·52H2O
Na9[(AsW9O33]·9H2O
Ophirite, Ca2Mg4[Zn2Mn2(H2O)2(FeW9O34)2]·46H2O